

**This is a self-archived version of an original article. This version may differ from the original in pagination and typographic details.**

**Author(s):** Guadilla, V.; Tain, J. L.; Algora, A.; Agramunt, J.; Jordan, D.; Monserrate, M.; Montaner-Pizá, A.; Orrigo, S. E. A.; Rubio, B.; Valencia, E.; Briz, J. A.; Cucoanes, A.; Estienne, M.; Fallot, M.; Le Meur, L.; Porta, A.; Shiba, T.; Zakari-Issoufou, A.-A.; Äystö, J.; Eronen, T.; Gorelov, D.; Hakala, J.; Jokinen, A.; Kankainen, A.; Kolhinen, V. S.; Koponen, J.; Moore, I. D.; Penttilä, H.; Pohjalainen, I.; Reinikainen, J.

**Title:** Determination of  $\beta$ -decay ground state feeding of nuclei of importance for reactor applications

**Year:** 2020

**Version:** Published version

**Copyright:** © 2020 American Physical Society

**Rights:** In Copyright

**Rights url:** <http://rightsstatements.org/page/InC/1.0/?language=en>

**Please cite the original version:**

Guadilla, V., Tain, J. L., Algora, A., Agramunt, J., Jordan, D., Monserrate, M., Montaner-Pizá, A., Orrigo, S. E. A., Rubio, B., Valencia, E., Briz, J. A., Cucoanes, A., Estienne, M., Fallot, M., Le Meur, L., Porta, A., Shiba, T., Zakari-Issoufou, A.-A., Äystö, J., . . . Sonzogni, A.A. (2020). Determination of  $\beta$ -decay ground state feeding of nuclei of importance for reactor applications. *Physical Review C*, 102(6), Article 064304. <https://doi.org/10.1103/physrevc.102.064304>

**Determination of  $\beta$ -decay ground state feeding of nuclei of importance for reactor applications**

V. Guadilla<sup>1</sup>,\* J. L. Tain, A. Algora,<sup>†</sup> J. Agramunt, D. Jordan, M. Monserrate, A. Montaner-Pizá,  
S. E. A. Orrigo, B. Rubio, and E. Valencia  
*Instituto de Física Corpuscular, CSIC-Universidad de Valencia, E-46071 Valencia, Spain*

J. A. Briz, A. Cucoanes, M. Estienne, M. Fallot, L. Le Meur, A. Porta, T. Shiba, and A.-A. Zakari-Issoufou  
*Subatech, IMT-Atlantique, Université de Nantes, CNRS-IN2P3, F-44307 Nantes, France*

J. Äystö, T. Eronen, D. Gorelov, J. Hakala, A. Jokinen, A. Kankainen, V. S. Kolhinen,<sup>‡</sup> J. Koponen, I. D. Moore, H. Penttilä,  
I. Pohjalainen, J. Reinikainen, M. Reponen, S. Rinta-Antila, K. Rytönen, V. Sonnenschein,<sup>§</sup> and A. Voss  
*University of Jyväskylä, FIN-40014 Jyväskylä, Finland*

L. M. Fraile and V. Vedia  
*Grupo de Física Nuclear & IPARCOS, Universidad Complutense de Madrid, CEI Moncloa, E-28040 Madrid, Spain*

E. Ganioglu  
*Department of Physics, Istanbul University, 34134 Istanbul, Turkey*

W. Gelletly  
*Department of Physics, University of Surrey, GU2 7XH Guildford, United Kingdom*

M. Lebois and J. N. Wilson  
*Institut de Physique Nucléaire d'Orsay, 91406 Orsay, France*

T. Martinez  
*Centro de Investigaciones Energéticas Medioambientales y Tecnológicas, E-28040 Madrid, Spain*

E. Nácher  
*Instituto de Estructura de la Materia, CSIC, E-28006 Madrid, Spain*

A. A. Sonzogni  
*NNDC, Brookhaven National Laboratory, Upton, New York 11973-5000, USA*

 (Received 20 May 2020; accepted 10 November 2020; published 2 December 2020)

In  $\beta$ -decay studies the determination of the decay probability to the ground state (g.s.) of the daughter nucleus often suffers from large systematic errors. The difficulty of the measurement is related to the absence of associated delayed  $\gamma$ -ray emission. In this work we revisit the  $4\pi\gamma - \beta$  method proposed by Greenwood and collaborators in the 1990s, which has the potential to overcome some of the experimental difficulties. Our interest is driven by the need to determine accurately the  $\beta$ -intensity distributions of fission products that contribute significantly to the reactor decay heat and to the antineutrinos emitted by reactors. A number of such decays have large g.s. branches. The method is relevant for nuclear structure studies as well. Pertinent formulas are revised and extended to the special case of  $\beta$ -delayed neutron emitters, and the robustness of the method is demonstrated with synthetic data. We apply it to a number of measured decays that serve as test cases and discuss the features of the method. Finally, we obtain g.s. feeding intensities with reduced uncertainty for four relevant decays that will allow future improvements in antineutrino spectrum and decay heat calculations using the summation method.

DOI: [10.1103/PhysRevC.102.064304](https://doi.org/10.1103/PhysRevC.102.064304)

\*Present address: Faculty of Physics, University of Warsaw, 02–093 Warsaw, Poland.

<sup>†</sup>Also at: Institute of Nuclear Research of the Hungarian Academy of Sciences, Debrecen H-4026, Hungary 4026, Hungary.

<sup>‡</sup>Present address: Cyclotron Institute, Texas A&M University, College Station, Texas 77843, USA.

<sup>§</sup>Present address: Faculty of Engineering, Nagoya University, Nagoya 464–8603, Japan.

## I. INTRODUCTION

The measurement of ground state (g.s.)  $\beta$ -decay feeding probabilities is hampered by the absence of associated  $\gamma$  radiation. In  $\beta^-$  decays the energy released is shared between the electron and the antineutrino leading to continuous energy distributions, extending from zero to the maximum decay energy  $Q_\beta$ . This makes it difficult to determine precisely the number of  $\beta$  particles. The problem arises because of the difficulty of disentangling the featureless continuum associated with all of the decays to excited states from that to the g.s. through  $\beta$ -spectrum deconvolution. In addition, electrons are easily absorbed or scattered by any material surrounding the  $\beta$  detector, and this effect must be properly taken into account in the response function of the  $\beta$  detector. This explains why  $\beta$ -decay probabilities to the g.s. are often obtained indirectly.

The most common approach is to determine both the total number of decays and the number of decays proceeding to excited states, since the difference is due to decays to the g.s. Usually the total number of decays is measured using a  $\beta$  detector and the decays to excited states are obtained from high-resolution (HR)  $\gamma$ -ray spectroscopy and conversion electron spectroscopy to build the decay level scheme. Assigning the correct intensity for the decay to the g.s. is equivalent to determining absolute  $\gamma$  intensities. The limited efficiency of HPGe detectors results in many weak transitions from levels at high-excitation energy remaining undetected, the so-called *pandemonium* effect [1]. This shifts the apparent  $\beta$  intensity, obtained from the intensity balance at each level, to levels at low-excitation energies. This in itself is not the real problem for g.s. feeding determination but the fact that part of the missed transitions can feed the g.s. directly, thus introducing a systematic error in the determination of absolute  $\gamma$  intensities. In a strict sense the g.s. feeding probabilities obtained by this method should be considered as upper limits.

Greenwood and collaborators [2] proposed the use of the pandemonium-free total absorption  $\gamma$ -ray spectroscopy (TAGS) technique [3] in combination with a  $\beta$  detector to determine accurately the  $\beta$  intensity to the g.s., in a way that will be explained later. The method, termed the  $4\pi\gamma - \beta$  method, was applied subsequently to determine the g.s. feeding probabilities for 34 fission products (FP) [4,5].

The TAGS technique aimed initially at the determination of (relative)  $\beta$  intensities to excited states. It relies on the use of large close-to- $4\pi$   $\gamma$  calorimeters made with scintillation material to detect the full deexcitation  $\gamma$  cascade rather than the individual transitions. An ideal total absorption spectrometer would have 100%  $\gamma$ -cascade detection efficiency and should be insensitive to  $\beta$  particles. It turns out that the TAGS technique can be used to extract the g.s.  $\beta$  intensity directly as is explained below.

The first spectrometer designs emphasized the condition of insensitivity to  $\beta$  particles, either by placing a  $\beta$  detector outside the spectrometer [6] or placing a low- $Z$  absorber material behind the  $\beta$  detector [7–9] to minimize the penetration of the electrons or their bremsstrahlung radiation (in short  $\beta$  penetration) in the scintillation volume. This had the undesirable effect of reducing the  $\gamma$ -peak detection efficiency. However,

the total detection efficiency for  $\gamma$  cascades of multiplicity 2 or higher remains close to 100% if the solid angle coverage is reasonably close to  $4\pi$ . The rationale behind these initial designs is that  $\beta$  penetration distorts the spectrometer  $\gamma$  response by introducing a high-energy tail. The spectrometer response to decays is needed in the TAGS analysis of real spectrometers to deconvolute the measured spectrum [10]. The response must be obtained by Monte Carlo (MC) simulations [11] and the consensus at that time was that an accurate simulation of  $\beta$ -particle interactions is more difficult than the simulation of  $\gamma$  interactions. Modern MC simulation codes like Geant4 [12], have greatly improved the description of low-energy electron interactions and provide a variety of tracking parameters to optimize the simulation and improve the accuracy (see, for example, Ref. [13]). Thus the newest spectrometer designs [14–16] do not make any special effort to minimize  $\beta$  penetration and have a sizable response to g.s. decays. In this way the deconvolution of TAGS spectra provides, in a natural manner, the intensity of decays to the g.s. The first example of this was the decay of  $^{102}\text{Tc}$  for which the TAGS analysis [17,18] confirmed the value of 92.9(6)% quoted in ENSDF [19] coming from HR spectroscopy. Over the past few years, many other examples have shown the potential of the TAGS technique to obtain g.s. feeding probabilities [20–27]. However, the TAGS deconvolution method has some limitations: (1) the difficulties in validating the shape of the MC simulations of the  $\beta$  penetration in the spectrometer (see discussion in Ref. [21]); (2) the indeterminacy that can arise for particular decay intensity distributions, as will be shown later for the case of  $^{103}\text{Tc}$ ; (3) the loss of sensitivity with decreasing g.s.  $\beta$  intensity; (4) the difficulty of separating transitions to states at very low excitation energy, due to the limited energy resolution; and (5) the proper quantification of the systematic uncertainties.

In the present work we revisit the  $4\pi\gamma - \beta$  method, which, as will be seen, is essentially free from problems (1) and (2) listed before and has different systematic uncertainties from the TAGS analysis. These differences mainly arise from the integral character of the  $4\pi\gamma - \beta$  method (that uses the total number of counts in the spectra) that contrasts with the TAGS deconvolution, sensitive to the features of the shape of the experimental spectrum. As will be shown later, this minimizes the effect of the lack of knowledge on the precise deexcitation paths (a relevant source of systematic uncertainty in the TAGS analyses) in the results of the  $4\pi\gamma - \beta$  method.

Our interest in this topic arises from the importance of g.s. feeding probabilities for nuclear structure studies and reactor applications. In particular, it was recently renewed by the need to obtain accurate antineutrino energy spectra emitted by FP using the  $\beta$ -intensity distributions  $I_\beta(E_x)$  to weight the individual  $\bar{\nu}_e$  spectra for each  $\beta$  end-point  $Q_\beta - E_x$ . This is the basis of the summation method to obtain the spectrum of antineutrinos emitted by a nuclear reactor [28], which is calculated by weighting the spectrum for each FP by the cumulative (or evolved individual) fission yield and the contribution of each fissile isotope. It is known that a number of fission products of significance in forming the reactor antineutrino spectrum have a strong or very strong g.s. decay branch [29]. Some of them are  $^{92}\text{Rb}$  [95.2(7)%],

$^{96\text{gs}}\text{Y}$  [95.5(5)%],  $^{142}\text{Cs}$  [56(5)%],  $^{100\text{gs}}\text{Nb}$  [50(7)%],  $^{140}\text{Cs}$  [35.9(17)%], or  $^{93}\text{Rb}$  [35(3)%]. Here the quoted g.s. feeding probability in brackets is coming from the Evaluated Nuclear Structure Data File (ENSDF) [30]. The importance of direct measurements of the g.s. feeding and the impact on antineutrino spectrum calculations can be illustrated with the example of  $^{92}\text{Rb}$ , the top contributor above  $E_{\bar{\nu}_e} = 5$  MeV [20,29], with  $Q_\beta = 8.095(6)$  MeV [31]. The evaluated g.s. feeding probability in the ENSDF database, based on HR spectroscopy, was 51(18)% [32] until 2012 when it changed to 95.2(7)% [33] as a result of a new measurement of  $\gamma$ -ray intensities [34]. From the deconvolution of the measured TAGS spectrum we obtained a value of 87.5(25)% [20], close to the last evaluation. This result was confirmed with the 91(3)% value obtained by the ORNL group (Fijałkowska *et al.*) [23] using the MTAS total absorption spectrometer. In both cases, a significant improvement of reactor antineutrino summation calculations using the pandemonium-free value obtained with the TAGS technique was reported [20,22].

An accurate knowledge of the antineutrino spectrum is key to the analysis of reactor antineutrino oscillation experiments. The standard method to obtain this spectrum is to apply a complex conversion procedure to integral  $\beta$  spectra for each of the main fissile isotopes in a reactor [35]. A reevaluation of the conversion procedure [36,37] led to the discovery of a deficit of about 6% between observed and estimated antineutrino fluxes [38]. This was termed the reactor antineutrino anomaly. Whether it indicates the existence of sterile neutrinos is a topic of very active investigation [39]. The summation method allows an exploration of the origin of the anomaly from a different perspective, and recently it was shown that the consistent inclusion of our newest TAGS decay data reduces the discrepancy with the measured flux to the level of the estimated uncertainties [40]. On the other hand the high statistics spectrum of detected antineutrinos obtained by the Daya Bay collaboration [41] shows without doubt shape deviations with respect to the converted spectra. Such shape deviations were also seen by the Double Chooz [42] and Reno [43] collaborations. The origin of this shape distortion is unclear but the use of summation calculations allows one to explore a number of possibilities [44]. Moreover, fine structure has been observed in the Daya Bay spectra that has been ascribed to a few nuclear species with large g.s. feeding on the basis of summation calculations [45]. This opens the unlooked-for possibility of doing reactor  $\bar{\nu}_e$  spectroscopy.

There is a related application in which the role of g.s. feeding values is also of great relevance: the evaluation of the energy released in nuclear reactors by the radioactive decay of the FP, known as decay heat. The decay heat represents the dominant source of energy when a reactor is powered off and its proper determination is essential for safety reasons. It is usually evaluated by means of summation calculations that use the same ingredients mentioned above: fission yields,  $\beta$ -intensity distributions, and  $\beta$  spectra as a function of end-point energies to compute the evolution of the reactor decay heat with time. Some important decays for the determination of the reactor decay heat exhibit relevant g.s.  $\beta$  branches (many of them are common cases with the

reactor antineutrino spectrum explained before). The accurate determination of the decay heat is thus constrained by the availability of reliable g.s. feeding probability values.

This paper is organized as follows. The  $4\pi\gamma - \beta$  method is presented in Sec. II, including a correction of the original formulas in Ref. [2]. In addition, a modification of the formulas for the case of  $\beta$ -delayed neutron emitters is introduced. In Sec. III we provide a demonstration of the method using synthetic data generated by realistic MC simulations. The  $4\pi\gamma - \beta$  method is applied to TAGS data taken at the Accelerator Laboratory of the University of Jyväskylä (JYFL) in Sec. IV. It gives a summary of relevant experimental details and presents the results obtained, first for a number of relevant test cases and then for a number of isotopes contributing significantly to reactor antineutrino spectra and decay heat. The g.s. intensities obtained are compared with the TAGS deconvolution results and the literature. The last section summarizes the conclusions.

## II. THE $4\pi\gamma - \beta$ METHOD

The method is based on a comparison of the number of counts detected in the  $\beta$  detector  $N_\beta$  and the number of counts registered in coincidence in both the  $\beta$  detector and the total absorption spectrometer  $N_{\beta\gamma}$ . These can be written in terms of the number of decays  $f_i$  feeding level  $i$ , with  $i = 0$  representing the g.s., and they are related to the  $\beta$  intensity  $I_\beta^i$  and the total number of decays  $N_d$ :

$$\begin{aligned} N_\beta &= \varepsilon_\beta^0 f_0 + \sum_{i>0} \varepsilon_\beta^i f_i \\ &= \varepsilon_\beta^0 I_\beta^0 N_d + \sum_{i>0} \varepsilon_\beta^i I_\beta^i N_d \\ N_{\beta\gamma} &= \varepsilon_{\beta\gamma}^0 f_0 + \sum_{i>0} \varepsilon_{\beta\gamma}^i f_i \\ &= \varepsilon_{\beta\gamma}^0 I_\beta^0 N_d + \sum_{i>0} \varepsilon_{\beta\gamma}^i I_\beta^i N_d, \end{aligned} \quad (1)$$

where  $\varepsilon_\beta^i$  is the probability of detecting a signal in the  $\beta$  detector for decays to level  $i$  and  $\varepsilon_{\beta\gamma}^i$  the probability of registering simultaneously signals in the  $\beta$  detector and the total absorption  $\gamma$ -ray spectrometer. As seen in Eq. (1) we have separated explicitly the g.s. contribution. Let us define average  $\beta$  efficiencies for decays to excited states only, both in singles  $\bar{\varepsilon}_\beta^*$  and in coincidence with the total absorption  $\gamma$ -ray spectrometer  $\bar{\varepsilon}_{\beta\gamma}^*$ ,

$$\begin{aligned} \bar{\varepsilon}_\beta^* &= \frac{\sum_{i>0} \varepsilon_\beta^i f_i}{\sum_{i>0} f_i} = \frac{\sum_{i>0} \varepsilon_\beta^i I_\beta^i}{1 - I_\beta^0} \\ \bar{\varepsilon}_{\beta\gamma}^* &= \frac{\sum_{i>0} \varepsilon_{\beta\gamma}^i f_i}{\sum_{i>0} f_i} = \frac{\sum_{i>0} \varepsilon_{\beta\gamma}^i I_\beta^i}{1 - I_\beta^0}. \end{aligned} \quad (2)$$

The reason for this somewhat artificial definition is that they are well determined from a TAGS analysis even in the specific cases when the spectrometer is insensitive to g.s.  $\beta$  penetration as will be shown later. Using these average

efficiencies Eq. (1) can be rewritten as:

$$\begin{aligned} \frac{N_\beta}{N_d} &= \varepsilon_\beta^0 I_\beta^0 + \bar{\varepsilon}_\beta^* (1 - I_\beta^0) \\ \frac{N_{\beta\gamma}}{N_d} &= \varepsilon_{\beta\gamma}^0 I_\beta^0 + \bar{\varepsilon}_{\beta\gamma}^* (1 - I_\beta^0), \end{aligned} \quad (3)$$

from which  $I_\beta^0$  can be determined:

$$I_\beta^0 = \frac{1 - \frac{N_{\beta\gamma}}{N_\beta} \frac{\bar{\varepsilon}_\beta^*}{\bar{\varepsilon}_{\beta\gamma}^*}}{1 + \frac{N_{\beta\gamma}}{N_\beta} \frac{\varepsilon_\beta^0 - \bar{\varepsilon}_\beta^*}{\bar{\varepsilon}_{\beta\gamma}^*} - \frac{\varepsilon_{\beta\gamma}^0}{\bar{\varepsilon}_{\beta\gamma}^*}}. \quad (4)$$

This Eq. (4) can be compared with the equivalent one [Eq. (13)] in the original publication of Greenwood *et al.* [2] that can be rewritten using our nomenclature as:

$$I_\beta^0 = \frac{1 - \frac{N_{\beta\gamma}^*}{N_\beta} \frac{1}{\bar{\varepsilon}_\gamma^*}}{1 + \frac{N_{\beta\gamma}^*}{N_\beta} \frac{\varepsilon_\beta^0 - \bar{\varepsilon}_\beta^*}{\bar{\varepsilon}_\gamma^* \bar{\varepsilon}_{\beta\gamma}^*}}. \quad (5)$$

In the conversion we have used the following equivalence to the notation of Greenwood *et al.*:  $\bar{\varepsilon}_\gamma^* = 1 - L$ ,  $\varepsilon_\beta^0 = f_{\text{gs}} \omega_\beta$ , and  $\bar{\varepsilon}_\beta^* = f_{\text{ex}} \omega_\beta$ . Even assuming that the factorization  $\bar{\varepsilon}_{\beta\gamma}^* = \bar{\varepsilon}_\beta^* \bar{\varepsilon}_\gamma^*$  is valid, there are differences between this expression and Eq. (4). A correction term is missing in the denominator and  $N_{\beta\gamma}^*$  represents  $N_{\beta\gamma}$  corrected by the  $\beta$  penetration for g.s. decays (with probability  $\varepsilon_{\beta\gamma}^0$ ) and for decays to excited states where the  $\gamma$  cascade is not detected in the spectrometer (with probability  $\tilde{\varepsilon}_{\beta\gamma}^i$ )  $N_{\beta\gamma}^* = N_{\beta\gamma} - \varepsilon_{\beta\gamma}^0 f_0 - \sum_{i>0} \tilde{\varepsilon}_{\beta\gamma}^i f_i$ . We show in Sec. III, using synthetic data, that Eq. (5) produces inconsistent results.

The application of the  $4\pi\gamma - \beta$  method requires the determination of the experimental ratio  $R = N_{\beta\gamma}/N_\beta$  and the estimation of three correction factors,  $a$ ,  $b$ , and  $c$ , that are ratios of  $\beta$  efficiencies,

$$I_\beta^0 = \frac{1 - aR}{1 + bR - c}. \quad (6)$$

From its expression [compare Eq. (6) with Eq. (4)] one can see that correction factor  $a$  is close to (but larger than) one, correction factor  $b$  is a small number (that can be both positive or negative), and correction factor  $c$  is a relative measure of  $\beta$  penetration for decays to the g.s. To estimate accurately the correction factors we need to know the dependency of  $\beta$  efficiency with end-point energy and the  $\beta$ -intensity distribution with excitation energy [see Eq. (2)]. Notice that only the relative  $\beta$  intensity to excited states is required. We also need to know the  $\beta$ -penetration probability in the total absorption  $\gamma$ -ray spectrometer. Since  $\gamma$  rays interact also in the  $\beta$  detector we must take this effect into account, which implies that we must have a knowledge of decay  $\gamma$  cascades. These are also needed to obtain the  $\beta$ - $\gamma$  detection efficiency. Conversion electrons are readily detected in the  $\beta$  detector affecting both the  $\beta$  counts and the decay detection efficiency, and this is another effect that must be considered. As a matter of fact, all of this information is required for the analysis of TAGS data or is the result of such analysis (see Sec. IV). The accuracy of the  $4\pi\gamma - \beta$  method depends on the accuracy of the ratio of counts  $R$  and on the accuracy with which we can determine the correction factors. The integrated counts  $N_\beta$  and  $N_{\beta\gamma}$  can be

obtained from the measured  $\beta$  and  $\beta$ - $\gamma$  spectra but corrections for contaminants should be applied. The identification and quantification of contaminants is an important ingredient of the TAGS analysis, therefore providing the necessary information for the evaluation of this correction. In summary the  $4\pi\gamma - \beta$  method relies on the deconvolution of TAGS data and becomes a natural extension of it.

The decay of  $\beta$ -delayed neutron emitters requires special consideration. In this case the  $\beta$ -intensity distribution is the sum of two contributions  $I_\beta(E_x) = I_{\beta\gamma}(E_x) + I_{\beta n}(E_x)$ . The first one  $I_{\beta\gamma}(E_x)$  refers to decays that populate levels in the daughter nucleus that then deexcite by emission of  $\gamma$  rays. This is the one determined by the TAGS analysis. The second one  $I_{\beta n}(E_x)$  refers to decays that populate levels above the neutron separation energy  $S_n$  which is then followed by the emission of one or more neutrons and eventually  $\gamma$  rays in the deexcitation of the final nucleus. This component can be obtained from the measured  $\beta$ -delayed neutron spectrum and a knowledge of the branching probability to the different levels in the final nucleus (see Ref. [21] for further details). By separating the two components in the second row of Eq. (1) we obtain:

$$N_{\beta\gamma} = \varepsilon_{\beta\gamma}^0 I_\beta^0 N_d + \sum_{i>0} \varepsilon_{\beta\gamma}^i I_{\beta\gamma}^i N_d + \sum_{i>0} \varepsilon_{\beta n\gamma}^i I_{\beta n}^i N_d. \quad (7)$$

The last term represents the counts coming from the interaction of the  $\beta$ -delayed neutrons with the total absorption  $\gamma$ -ray spectrometer which is another source of contamination in the TAGS analysis that must be corrected for as explained later. After eliminating this contribution the second row in Eq. (1) becomes  $N_{\beta\gamma} = \varepsilon_{\beta\gamma}^0 I_\beta^0 N_d + \sum_{i>0} \varepsilon_{\beta\gamma}^i I_{\beta\gamma}^i N_d$ . With a redefinition of the coincidence detection efficiency averaged over excited levels [second row of Eq. (2)]:

$$\bar{\varepsilon}_{\beta\gamma}^* = \frac{\sum_{i>0} \varepsilon_{\beta\gamma}^i I_{\beta\gamma}^i}{1 - I_\beta^0}, \quad (8)$$

we arrive formally to the same formula Eq. (4) to calculate  $I_\beta^0$ . Notice, however, that now  $\bar{\varepsilon}_\beta^*$  is calculated with the total  $\beta$ -intensity distribution  $I_\beta^i$  while  $\bar{\varepsilon}_{\beta\gamma}^*$  is calculated with the partial intensity distribution  $I_{\beta\gamma}^i$ . The latter is normalized to  $1 - P_n$  instead of 1. This introduces a difference in the formulas for the decay of  $\beta$ -delayed neutron emitters in addition to the subtraction from  $N_{\beta\gamma}$  of the counts coming from the interaction of the  $\beta$ -delayed neutrons with the total absorption  $\gamma$ -ray spectrometer. Such an extension of the formulas for  $\beta$ -delayed neutron emitters was not discussed in the work of Greenwood *et al.*

In the next section we apply the method to synthetic data to demonstrate the consistency of the formulas and investigate its performance. In Sec. IV we apply the method to experimental data for a number of selected isotopes that either show some particularities in the use of the method or are important in determining the reactor antineutrino spectrum and/or the reactor decay heat.

### III. APPLICATION TO SYNTHETIC DATA

The synthetic data emulate the decay of  $^{87}\text{Br}$ ,  $^{88}\text{Br}$ , and  $^{94}\text{Rb}$ , that we have previously investigated with the TAGS

technique [21]. From the deconvolution of TAGS spectra we obtained g.s. feeding intensities of  $10.10^{+1.19}_{-0.94}\%$  and  $4.72^{+1.03}_{-2.19}\%$  for  $^{87}\text{Br}$  and  $^{88}\text{Br}$ , respectively. By comparison, ENSDF assigns a decay intensity to the g.s. of 12.0(19)% in the first case [46] and an upper limit of 11% in the second case [47]. The g.s.  $\rightarrow$  g.s. decay in  $^{94}\text{Rb}$  corresponds to a third forbidden transition with negligible intensity. These three nuclei are  $\beta$ -delayed neutron emitters with neutron emission probabilities of 2.43(14)%, 6.75(18)%, and 10.24(21)%, respectively [48]. For simplicity we have not included this decay channel in the simulation since we are interested here in testing the performance of the method. Accordingly only one  $\beta$ -intensity distribution (normalized to 1) is used to calculate the correction factors in Eq. (4) (Sec. II) and we need to scale by  $1 - P_n$  the  $I_\beta^0$  obtained in order to compare with the true value, defined as the input value for the simulation.

The measurement was performed using a compact 12-fold segmented  $\text{BaF}_2$  total absorption spectrometer with cylindrical shape and a thin Si detector placed close to the source position subtending a solid angle fraction of  $\approx 30\%$  as described in Ref. [21]. Spectra were simulated with the Geant4 Simulation Toolkit [12] implementing the detailed description of the setup and using decay cascades produced by the DECAyGEN event generator [49]. The inputs to the event generator are the branching ratio matrix used in the TAGS analysis and the resulting  $\beta$ -intensity distribution that was adopted as the final solution in Ref. [21]. This provides a very realistic simulation of the decay and its detection. In the simulation, as well as in the analysis, we assume that all  $\beta$ -energy distributions have an allowed shape. The reconstruction of the energy deposited in the event mimics that of the experiment. The experimental low energy threshold of 65 keV is applied to each spectrometer segment before summing to obtain the total energy deposited. Similarly, a threshold (in both MC and experiment) of 105 keV is applied to the Si detector before gating on the spectrometer signals.

In the top panel of Fig. 1 the spectrum of energy deposited in the spectrometer, with and without the  $\beta$ -gating condition, and the spectrum of energy deposited in the Si detector are shown for the case of the decay of  $^{87}\text{Br}$ . The instrumental resolution is switched off in these spectra to show more clearly their features. One million decay events were simulated. The total number of counts in the ungated TAGS spectrum is  $0.890 \times 10^6$  and  $0.255 \times 10^6$  in the gated spectrum. The counts in the Si detector spectrum are  $0.288 \times 10^6$ . The lower panel of Fig. 1 shows the simulated detection efficiency of the Si detector as a function of excitation energy together with the simulated probability of registering a signal simultaneously in the Si detector and the  $\gamma$  spectrometer. The pronounced efficiency drop above  $E_x = 5$  MeV is due to the low energy threshold in the Si detector and the continuum nature of  $\beta$  spectra. The decrease of the spectrometer-gated Si detector efficiency below 5 MeV in comparison with the ungated efficiency is due to the importance in this decay of deexcitations proceeding by a single  $\gamma$  transition to the g.s., which have a greater probability of escaping detection in the spectrometer. Using these efficiency distributions and Eq. (2) we can calculate the correction factors for each decay and apply Eq. (6) to obtain  $I_\beta^0$ .

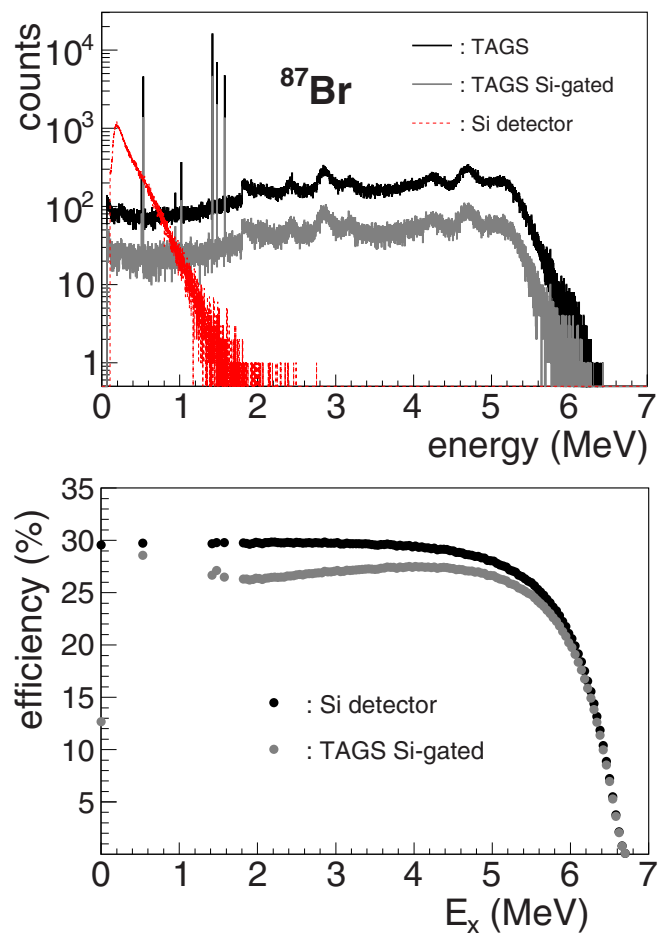


FIG. 1. Top panel: simulated Si detector spectrum (red dashed line) and TAGS spectra with (gray line) and without (black line) gating on Si signals for the decay of  $^{87}\text{Br}$ . The instrumental resolution is not included in these spectra. Bottom panel: simulated  $\beta$  efficiency without (black symbols) and with (gray symbols) a gating condition on the  $\gamma$  spectrometer. See text for further details.

The results of the calculation for the three isotopes are presented in Table I. As can be observed the value obtained for the g.s. feeding probability (10.12%, 4.79%, and 0.11% for  $^{87}\text{Br}$ ,  $^{88}\text{Br}$ , and  $^{94}\text{Rb}$ , respectively) is very close to the true value (i.e., the input values for the simulation) in all cases (10.10%, 4.72%, 0%). If the original formula from Greenwood *et al.* [Eq. (5)] is used, with  $N_{\beta\gamma}$  corrected for the  $\beta$  penetration, then we obtain 8.08%, 3.69%, and 0.28%, respectively, which deviate clearly from the true values for

TABLE I. Ratio of counts  $R$ , correction factors  $a$ ,  $b$ , and  $c$  and calculated  $\beta$  intensity to the g.s. for synthetic data. See text for further details.

Isotope	$R$	$a$	$b$	$c$	$I_\beta^0$ (%)
$^{87}\text{Br}$	0.8846	1.064	$4.91 \times 10^{-2}$	0.477	10.12
$^{88}\text{Br}$	0.9444	1.038	$-1.67 \times 10^{-3}$	0.608	4.79
$^{94}\text{Rb}$	0.9913	1.008	$-9.83 \times 10^{-3}$	0.656	0.11

the bromine isotopes. From the values of the correction factor  $c$  we can see that in this setup the  $\gamma$  spectrometer is rather sensitive to  $\beta$  penetration for decays to the g.s., between 48% and 66% of the average probability of detecting a decay to an excited state. The increase in  $c$  with isotope follows the increase in  $Q_\beta$ .

Another important check that can be performed with the synthetic data is to test the stability of the result against uncertainties in the deconvolution procedure. As explained in Ref. [21] the  $\beta$ -intensity distribution obtained in the TAGS analysis is affected by several systematic uncertainties related to the branching ratio matrix used to build the spectrometer response, the accuracy of the MC simulations, the normalization of contaminants and even the deconvolution method. This results in a spread of  $I_\beta^0$  extracted from the deconvolution method which varied between 9.16% and 11.29% (14 intensity distributions) for  $^{87}\text{Br}$ , and between 2.60% and 5.82% (13 intensity distributions) for  $^{88}\text{Br}$ . Actually this spread determines the size of the systematic uncertainty of the g.s. feed obtained from the deconvolution method quoted above. In comparison the statistical uncertainty from deconvolution is negligible (below 0.05%). However, if we use the different  $\beta$ -intensity distributions to calculate the correction factors  $a$ ,  $b$ , and  $c$  and apply the  $4\pi\gamma - \beta$  method to the synthetic spectra simulated with the adopted  $I_\beta$  distribution (shown in the top panel of Fig. 1 for the  $^{87}\text{Br}$  case) the resulting  $I_\beta^0$  vary very little. For example, in the deconvolution of  $^{87}\text{Br}$  data, we tested the effect of fixing the g.s. feeding probability to the ENSDF value 12%. This resulted in a still acceptable fit to the data, just outside the 5% maximum increase in  $\chi^2$  that was used to select the set of acceptable solutions in the original publication [21]. When using the resulting  $\beta$  intensity to calculate the correction factors in Eq. (6) we obtain  $I_\beta^0 = 10.17\%$  very close to the true value. Likewise, in the case of  $^{88}\text{Br}$  we tested the effect in the deconvolution of fixing the g.s. feeding probability to 11%, which is the upper limit given by ENSDF. In this case the fit to the data was rather poor (44% increase in  $\chi^2$ ) as expected. In spite of that, when we use the resulting  $\beta$ -intensity distribution to calculate the g.s. feeding probability in the  $4\pi\gamma - \beta$  method it gives 4.78%, close to the true value. This simply reflects the fact that the TAGS technique determines rather accurately the relative  $\beta$  intensity to excited states that proceed by  $\gamma$ -ray emission, on which the correction factors are based. In other words, the  $4\pi\gamma - \beta$  method is much less sensitive to the systematic uncertainties in the deconvolution of TAGS data. An extreme example is presented in Sec. IV A.

#### IV. EXPERIMENTAL RESULTS

A campaign of TAGS measurements was carried out in 2014 at the upgraded Ion Guide Isotope Separator On-Line (IGISOL) IV facility [50] at the University of Jyväskylä. One of the motivations for these measurements was to improve both reactor decay heat and antineutrino spectrum summation calculations, by providing data free from the pandemonium effect for some nuclei having significant g.s. feeding values. In the experiment we employed the 18-fold segmented NaI(Tl)

Decay Total Absorption  $\gamma$ -ray Spectrometer (DTAS) [15] in coincidence with a 3-mm-thick plastic scintillation detector. This  $\beta$  detector was located at the center of DTAS and in front of a movable tape for the implantation of the nuclei of interest and the removal of the daughter activity (see Ref. [51] for more details about the experiment). The mean efficiency of the  $\beta$  detector is around 30% for end-point energies above 2 MeV (see Fig. 1 for a similar detector), while the efficiency for  $\beta$  particles of DTAS in coincidence with the  $\beta$  detector ranges from 1% at 4-MeV  $\beta$  end-point energy to 5% at 8 MeV [52].

We provide in the following a brief description of TAGS data analysis for the reader's better understanding. The  $\beta$ -gated total energy deposited in DTAS was reconstructed off-line from the signals of the individual detector modules as described in Ref. [52], with threshold values of 90 keV for DTAS modules and 70 keV for the  $\beta$  detector. The coincidence between DTAS and the  $\beta$  detector allowed us to get rid of the environmental background. Other sources of contamination need to be accounted for. These include in general the activity of the descendants. For each descendant that contributes significantly we measure the shape of its energy spectra or, in the case of well-known decays, we obtain it through MC simulations using the available decay data. If possible the normalization of these spectra is obtained by adjustment to salient features on the measured parent decay spectra that can be identified as due to the descendant activity, otherwise from the relation of parent-descendant half-lives. In the case of  $\beta$ -delayed neutron emitters, as mentioned above, the  $\beta$ -delayed neutron branch introduces an additional contamination that includes the interaction of neutrons with DTAS. The shape of the contaminant spectrum is obtained by MC simulation following a special procedure detailed in Ref. [21] and the normalization is obtained by adjustment to the measured spectra, if possible, otherwise it is given by the  $P_n$  value. We also take into account the electronic pulse summing-pileup effect that contributes to the distortion of the spectra. The need to consider two components (summing and pileup) is particular to multidetector systems. The pileup originates in the superposition of different event signals in the same detector module within the analog-to-digital converter (ADC) time gate. The summing is due to the sum of signals corresponding to different events that are detected in different modules within the same ADC gate. The summing-pileup contribution is calculated by means of a MC sampling method [52] specifically developed for segmented spectrometers. The calculated spectrum is normalized from the detection rate and the length of the ADC gate [52].

In order to determine the  $\beta$  intensities from TAGS experimental spectra, we followed the method developed by the Valencia group [10,11,49]. For this, one has to solve the inverse problem  $d_i = \sum_j R_{ij}(B)f_j + C_i$ , where  $d_i$  represents the number of counts in channel  $i$  of the spectrum,  $f_j$  is the number of events that feed level  $j$  in the daughter nucleus,  $R_{ij}$  is the response function of the spectrometer, which depends on the branching ratios ( $B$ ) for the different deexcitation paths of the states populated in the decay, and  $C_i$  is the sum of all contaminants at channel  $i$ .

To build the spectrometer response to decays we need the response to individual  $\gamma$  rays and  $\beta$  particles [11]. These

are obtained from MC simulations using a very detailed description of the measurement setup (including electronic thresholds), carefully benchmarked with laboratory sources. We also need the branching ratio matrix describing the de-excitation pattern as a function of level excitation energy, including the conversion electron process. This is obtained from the HR spectroscopy level scheme at low excitation energies supplemented with the predictions of the Hauser-Feshbach nuclear statistical model above a given excitation energy where the levels are treated as a binned continuum [49]. The statistical model provides a realistic description of the electromagnetic cascade energy and multiplicity distribution, that in modern segmented spectrometers can be tested as well [26,27,53] and eventually modified.

Finally, the TAGS spectrum deconvolution is carried out by applying a suitable algorithm, which in the present case is the expectation maximization algorithm, to extract the  $\beta$ -feeding distribution [10].

In order to apply the  $4\pi\gamma - \beta$  method to obtain  $I_\beta^0$  we must determine the experimental number of counts  $N_{\beta\gamma}$  and  $N_\beta$ .  $N_{\beta\gamma}$  is obtained from the number of counts in the  $\beta$ -gated DTAS spectrum after correction for the counts due to the contaminants. As we mentioned in Sec. II this correction follows closely the one applied to TAGS spectra for deconvolution since the contamination counts are determined by integration of the corresponding TAGS contamination spectra that we just described. In this line, the counts due to the activity of the descendants and, if needed, the  $\beta$ -delayed neutron branch contribution are subtracted. In the case of the summing-pileup contribution the counts are *added* since each count in the summing-pileup spectra represents the loss of two events. The uncertainty of  $N_{\beta\gamma}$  is estimated by considering the uncertainties in the normalization factors of the different components, taken from the TAGS analysis. Note that in all cases we integrate the full  $\beta$ -gated DTAS spectra, since experimental thresholds are already taken into account when requiring the  $\beta$ -gating condition, as mentioned above. The experimental thresholds are also taken into account in the MC efficiencies employed for the determination of coefficients  $a$ ,  $b$ , and  $c$  of Eq. (6).

$N_\beta$  is calculated as the number of counts in the spectrum of the  $\beta$  plastic detector above the threshold without any coincidence condition. In addition to the counts due to descendants, which are estimated from the TAGS analysis, in this case we also need to subtract environmental background counts, although this is a small amount. They are obtained from measurements without beam and normalized by the relative measurement times. The counts lost by electronic pulse pileup are added to the result. In this case, since we are dealing with a single detector, the calculation and normalization of the pileup contribution is performed as in Ref. [54]. The uncertainty on  $N_\beta$  comes from the uncertainties in the normalization factors of the contaminants. For the environmental background we take a 20% uncertainty, which is the maximum deviation observed in tests with laboratory sources, while for the rest of the contaminants we take the same uncertainties used for the TAGS analysis.

Finally we should mention that in general the ratio  $N_{\beta\gamma}/N_\beta$  needs to be corrected for differences in the data acquisition

TABLE II. g.s. feeding intensities for a few decays of interest. The values obtained by the  $4\pi\gamma - \beta$  method are compared with results from the TAGS analysis and from evaluations in the ENSDF database [30].

Isotope	$I_\beta^0$ (%)		
	ENSDF	TAGS	$4\pi\gamma - \beta$
$^{95}\text{Rb}$	$\leq 0.1$	$0.03_{-0.02}^{+0.11}$	$-0.2(42)$
$^{100\text{gs}}\text{Nb}$	50(7)	$46_{-15}^{+16}$	40(6)
$^{102\text{m}}\text{Nb}$	—	$42.5_{-10.0}^{+9.3}$	44.3(28)
$^{100}\text{Tc}$	93.3(1)	93.9(5)	92.8(5)
$^{103}\text{Tc}^a$	34(8)	—	$45.6_{-0.9}^{+1.5}$
$^{137}\text{I}$	45.2(5)	$50.8_{-4.3}^{+2.7}$	45.8(13)
$^{140}\text{Cs}$	35.9(17)	$39.0_{-6.3}^{+2.4}$	36.0(15)

<sup>a</sup>For this decay the  $I_\beta^0$  numbers include the intensity to the first excited state in  $^{103}\text{Ru}$  at 2.81(5) keV.

dead times. In the present case this is not necessary because of the way our acquisition system works: every acquisition channel is gated with a common gate signal which is an OR of all individual detector triggers.

The results of the application of the  $4\pi\gamma - \beta$  method to part of the data obtained in the 2014 measurement campaign are presented below. First, cases of particular interest showing how the method works (Secs. IV A and IV B) and, second (Sec. IV C), cases that are of relevance for reactor antineutrino summation calculations. They are summarized in Table II. We note that errors quoted in Table II for the  $4\pi\gamma - \beta$  values are the quadratic sum of two contributions: (1) the uncertainty in the calculation of the ratio of counts  $R$  (the dominant contribution), which combines statistical uncertainties and uncertainties in the correction for contaminants and (2) the small contribution coming from the application of the method with all  $\beta$  intensity distributions used to estimate the error budget of the TAGS analyses. As mentioned before, we use the relative  $\beta$  intensities from the TAGS analyses as ingredients to evaluate the correction factors  $a$ ,  $b$ , and  $c$  from Eq. (4). The uncertainty in these correction factors can be estimated by computing them for all  $\beta$ -intensity distributions that give an acceptable reproduction of the TAGS experimental spectrum. As explained in detail in Ref. [21] each of these  $\beta$ -intensity distributions obtained in the TAGS analysis takes into account the effect of several systematic uncertainties related to the branching ratio matrix used to build the spectrometer response, to the accuracy of MC simulations, to the normalization of contaminants and even to the deconvolution method employed. As discussed in Sec. III for the synthetic data, the influence of the  $\beta$ -intensity distribution in the correction factors  $a$ ,  $b$ , and  $c$  is very small, which is also related to the fact that the uncertainties in the average efficiencies defined in Eq. (2) are small.

#### A. The case of $^{103}\text{Tc}$

One of the cases studied is the decay of the  $5/2^+$  g.s. of  $^{103}\text{Tc}$  into  $^{103}\text{Ru}$  with a  $Q_\beta$  value of 2663(10) keV [31].



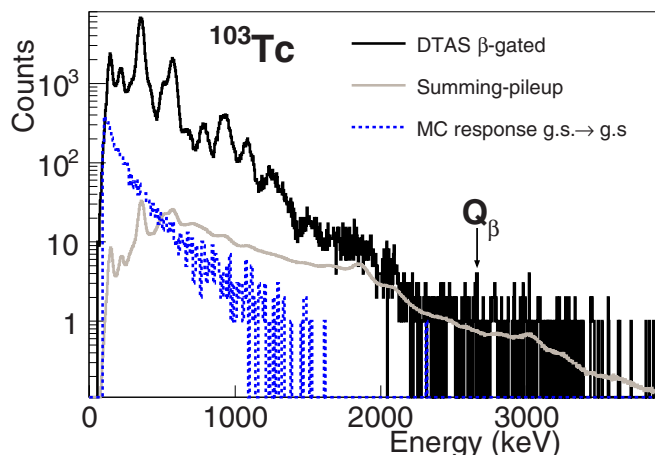


FIG. 2. Experimental  $\beta$ -gated spectrum (solid black) compared with the MC response of DTAS for the transition to the g.s. of  $^{103}\text{Ru}$  (dotted blue). The normalized summing pileup contribution is also shown (gray).

This TAGS measurement was assigned first priority for the prediction of the reactor decay heat with U/Pu fuel and second priority for Th/U fuel by the IAEA [55]. In addition to the  $3/2^+$  g.s. of the daughter nucleus, the decay also populates a  $5/2^+$  state at only 2.81(5)-keV excitation energy, as observed in a previous HR spectroscopy experiment [56]. Since we are not able to separate the two close-lying states we refer to their summed decay intensity as the g.s. intensity  $I_{\beta}^0$ . The DTAS and  $\beta$ -detector spectra for this measurement are shown in Fig. 2 and Fig. 3 respectively, together with the spectra of the contaminants. Since  $^{103}\text{Ru}$  is very long lived ( $T_{1/2} = 39.2$  days) these are limited to the summing-pileup in the first case and the pileup and environmental background in the second case.

It turns out that  $^{103}\text{Tc}$  is a special case. In the TAGS analysis presented in Ref. [57], we found that the reproduction of the measured DTAS spectrum is almost insensitive to the value of the g.s. feeding intensity, which is an unusual situa-

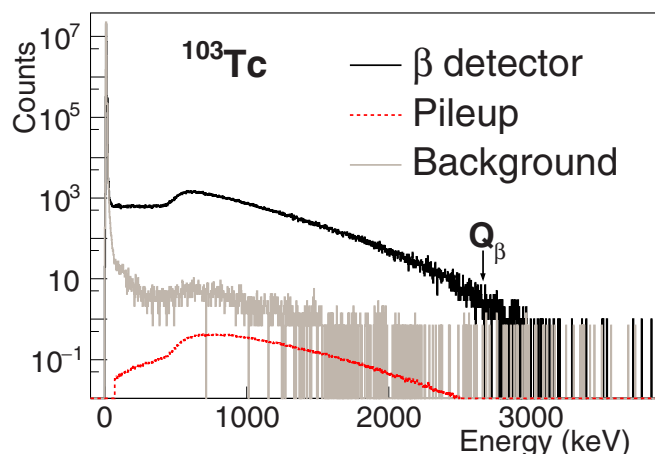


FIG. 3. Spectrum in singles of the plastic  $\beta$  detector for the decay of  $^{103}\text{Tc}$  (solid black line). The contaminants are shown with the appropriate normalization.

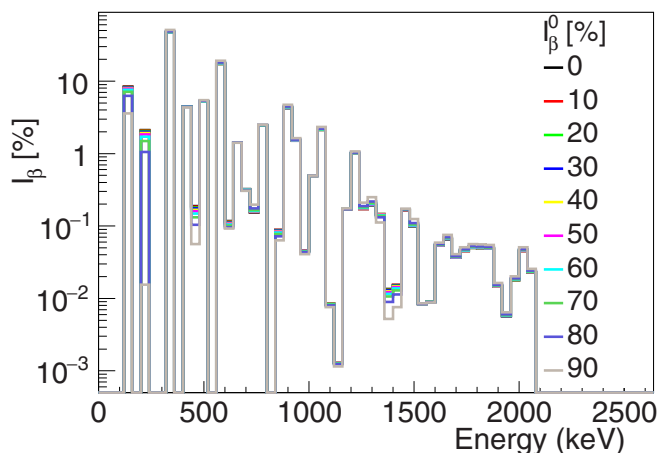


FIG. 4. Relative  $\beta$  intensities populating the excited states of  $^{103}\text{Ru}$  in the decay of  $^{103}\text{Tc}$ . The  $\beta$  intensities to excited states obtained from the TAGS analysis for different fixed values of  $I_{\beta}^0$  are normalized to  $1-I_{\beta}^0$ .

tion. The issue cannot be exclusively attributed to the low  $Q_{\beta}$  value of the decay, associated with a small detection efficiency of decays to the g.s. ( $\beta$  penetration), as demonstrated in the case of the decay of  $^{100}\text{Tc}$  ( $Q_{\beta} = 3206.4(14)$  [31]) presented in Sec. IV B. To illustrate this in Fig. 4 we show a set of relative  $\beta$  intensity distributions to excited states of  $^{103}\text{Ru}$ , each of them determined in a TAGS analysis with the g.s.  $\beta$  intensity fixed to a value between 0% and 90% in steps of 10%. The  $\beta$  intensity distribution obtained for each value of  $I_{\beta}^0$  is renormalized to the value of  $1-I_{\beta}^0$  in order to be able to compare the shape of relative  $\beta$ -intensity distributions to the excited states. As can be observed the resulting relative  $\beta$  intensities are almost unchanged when the value of the  $\beta$  intensity to the g.s. is fixed in the range 0% to 80%. For a value of 90% there is a sizable effect on the  $\beta$  intensity to states below 300 keV. The different  $I_{\beta}^0$  values fixed in the analysis introduce a change of around 15% in the  $\chi^2$  of the TAGS analysis (see Fig. 5), with a minimum at 70–80%. In other words, in this particular case one should not trust the TAGS analysis to obtain the g.s. feeding probability. The reason for this insensitivity is to be found in the shape of the response for the g.s. to g.s. transition. As shown in Fig. 2 the energy dependence of the MC simulated response for this transition happens to be similar to the overall shape of the total absorption experimental spectrum, thus the deconvolution algorithm is not very sensitive to the g.s. contribution.

We turn now to the  $4\pi\gamma - \beta$  method. We obtain a ratio of counts  $R$  of 0.495(5) for the decay of  $^{103}\text{Tc}$  and we use Eq. (4) to obtain  $I_{\beta}^0$ . As we have shown in Fig. 4, the reproduction of the TAGS experimental spectrum for the decay of  $^{103}\text{Tc}$  is compatible with a wide range of absolute  $\beta$ -intensity distributions. In contrast with such a lack of definition for this peculiar case, in Fig. 5 we obtain very stable results with the  $4\pi\gamma - \beta$  method when the  $\beta$ -intensity distributions of Fig. 4 are employed in the determination of the correction factors of Eq. (4), since only relative  $\beta$  intensities are involved. For this pathological case, we have chosen the average of

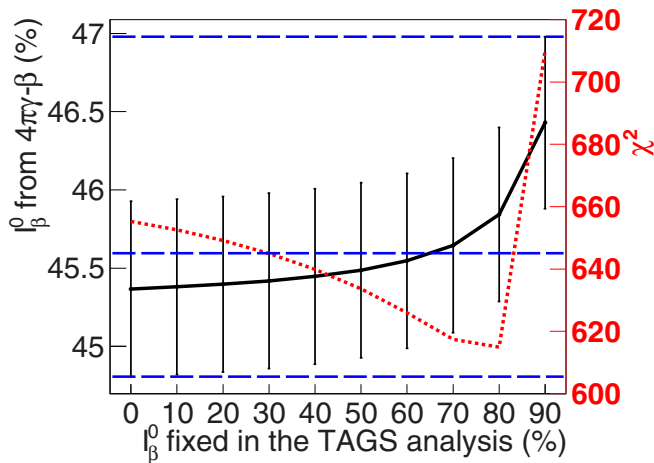


FIG. 5.  $I_{\beta}^0$  values obtained with the  $4\pi\gamma - \beta$  method for different  $\beta$ -intensity distributions determined from TAGS analyses performed with  $I_{\beta}^0$  fixed to values between 0 and 90% (solid black). The  $\chi^2$  of each TAGS analysis is shown in dotted red. The horizontal dashed blue line shows the mean  $I_{\beta}^0$  value. The upper and lower limits considered for the uncertainty are represented by horizontal dotted gray lines.

all values from Fig. 5,  $45.6_{-0.9}^{+1.5}\%$ , as our result for the g.s. to g.s.  $\beta$  intensity of the decay of  $^{103}\text{Tc}$ . The uncertainty is a conservative estimate based on the lowest and highest uncertainty deviations. This result is compatible with the value 41(10)% obtained in the HR spectroscopy work of Niizeki *et al.* [56]. However, it is larger than the 34(8)% value reported in the ENSDF evaluation [58] based also on HR spectroscopy studies. The difference between both is related to the adopted intensity of the 346.4 keV  $\gamma$  ray used for normalization: Niizeki *et al.* uses an intensity of 16% for this  $\gamma$  ray, whereas the ENSDF evaluation uses a value of 18.4% obtained in a fission yield measurement [59]. This example shows one of the difficulties faced when assigning g.s. feeding probabilities in HR spectroscopy.

We also use the decay of  $^{103}\text{Tc}$  to perform an illustrative exercise showing the dependence of the uncertainty of  $I_{\beta}^0$  in the  $4\pi\gamma - \beta$  method with  $I_{\beta}^0$  for a fixed value of the uncertainty in  $R$ . The  $\beta$ -intensity distributions obtained in the TAGS analysis with fixed  $I_{\beta}^0$  values between 10% and 90% (shown in Fig. 4) have been used as input to MC simulations of DTAS and plastic scintillation spectra (see Sec. III). The  $4\pi\gamma - \beta$  method was then applied to these spectra. The uncertainty in the ratio of counts  $R$  was fixed to 1%, the value of the current measurement. As shown in Fig. 6, the relative error in the determination of the g.s. feeding probability with the  $4\pi\gamma - \beta$  method varies between 10% at  $I_{\beta}^0 = 10\%$  and 1% at  $I_{\beta}^0 = 90\%$ . Thus the precision of the method is severely limited by statistics at low values of the g.s. feeding intensity.

### B. Cases with extreme values of the g.s. feeding intensity

The  $4\pi\gamma - \beta$  method has been applied to other test cases measured in the same DTAS experimental campaign. In those

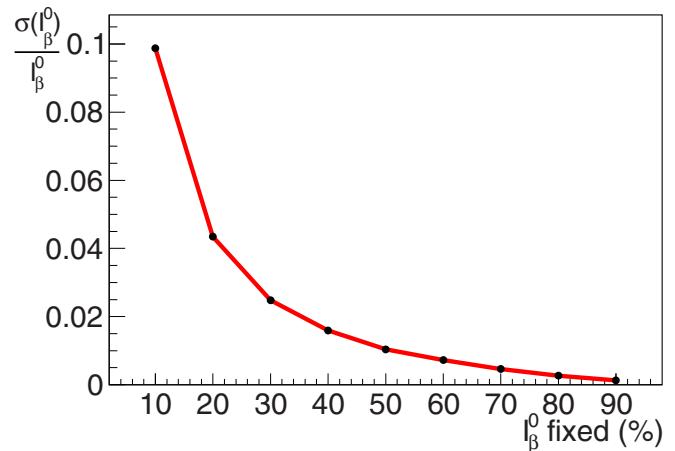


FIG. 6. Relative uncertainty of the  $I_{\beta}^0$  values obtained with the  $4\pi\gamma - \beta$  method applied to MC simulations. The TAGS results obtained with  $I_{\beta}^0$  fixed to different values from 10 to 90% in the analysis of the decay of  $^{103}\text{Tc}$  have been used as input for the event generator employed in the simulations. The uncertainty in the ratio of counts  $R$  was kept fixed at the experimental 1% value.

cases the TAGS analyses did show a sensitivity to the g.s. to g.s. transition, thus allowing us to compare the  $I_{\beta}^0$  determined from the deconvolution with the value obtained by means of the  $4\pi\gamma - \beta$  counting method presented here. In particular two cases are included here due to the extreme character of their g.s. feeding probability and importance: the decay of  $^{95}\text{Rb}$ , a  $\beta$ -delayed neutron emitter where the first forbidden  $5/2^- \rightarrow 1/2^+$  g.s. to g.s. transition is hindered, and the decay of  $^{100}\text{Tc}$ , dominated by the large Gamow-Teller  $1^+ \rightarrow 0^+$  g.s. to g.s. branch.

In the first case, the decay of  $^{95}\text{Rb}$ , we obtain an almost zero g.s. to g.s. feeding from TAGS analysis, in agreement with previous HR spectroscopy measurements [27] (see Table II). Nevertheless, our TAGS analysis shows that the HR data are affected by a strong pandemonium effect [27]. The  $4\pi\gamma - \beta$  method determines also a  $I_{\beta}^0$  value that is almost zero, though the relative uncertainty is large, as can be expected from the discussion in the previous section. In fact (see Table II) in this case the uncertainty is much larger than that determined by TAGS spectrum deconvolution. Due to the relatively small fission yield of  $^{95}\text{Rb}$ , the impact of our TAGS results in reactor antineutrino spectrum calculation is less than 1% between 7 and 9 MeV. For the same reason, in spite of being assigned first priority for the U/Pu fuel decay heat [55], the impact of these TAGS results is also subpercent on the electromagnetic component of the reactor decay heat of  $^{235}\text{U}$  and  $^{239}\text{Pu}$  for times shorter than 1 s [27].

In the second case, the decay of  $^{100}\text{Tc}$ , of interest for nuclear structure, a large  $I_{\beta}^0$  value of 93.9(5)% is determined from the TAGS spectrum deconvolution. As described in Ref. [60] a different  $\beta$  detector was employed in this measurement, which consists of a vase-shaped thin plastic scintillator with close-to- $4\pi$  solid angle coverage. The value of  $I_{\beta}^0$  obtained with the TAGS technique is compatible with the previous value from HR measurements (see Ref. [24] for

TABLE III. Contribution in percentage of the selected cases to the reactor antineutrino spectra of  $^{235}\text{U}$  and  $^{239}\text{Pu}$  at different energy ranges (based on the Nantes summation method [20]).

Isotope	3–4 MeV (%)		4–5 MeV (%)		5–6 MeV (%)	
	$^{235}\text{U}$	$^{239}\text{Pu}$	$^{235}\text{U}$	$^{239}\text{Pu}$	$^{235}\text{U}$	$^{239}\text{Pu}$
$^{100\text{gs}}\text{Nb}$	3.5	4.5	5.3	7.6	5.8	9.0
$^{102\text{m}}\text{Nb}$	0.7	1.5	0.7	1.7	0.4	1.0
$^{137}\text{I}$	1.7	1.6	2.2	2.3	2.0	2.3
$^{140}\text{Cs}$	2.8	2.9	3.3	3.7	2.5	3.0

a detailed discussion). The  $4\pi\gamma - \beta$  method gives a value of 92.8(5)% in agreement with the value from the TAGS analysis, thus confirming this important result. In this case the value quoted by ENSDF is in agreement within the uncertainties with both results. The  $\beta$ -intensity distribution of  $^{100}\text{Tc}$  decay serves as a benchmark for theoretical estimates of the nuclear matrix elements (NME) in the  $A = 100$  system that enter into the calculation of the double  $\beta$ -decay process in  $^{100}\text{Mo}$ . NME represent the largest uncertainty in the half-life estimate of the neutrino-less branch, thus limiting our ability to extract information on this process beyond the standard model.

### C. Reactor antineutrino spectrum cases

The remaining cases presented here are decays of fission fragments contributing significantly to the reactor antineutrino spectrum:  $^{100\text{gs}}\text{Nb}$ ,  $^{102\text{m}}\text{Nb}$ ,  $^{137}\text{I}$ , and  $^{140}\text{Cs}$ . Table III provides the percent contribution of the four isotopes to the total antineutrino spectrum for both  $^{235}\text{U}$  and  $^{239}\text{Pu}$  fission in three  $E_{\bar{\nu}_e}$  energy intervals covering the range from 3 to 6 MeV. These percentages were calculated using the Nantes summation method [20]. All cases listed in Table III have been assigned a first priority for TAGS measurement in the IAEA report [55], while  $^{137}\text{I}$  and  $^{100\text{gs}}\text{Nb}$  are also considered high-priority cases for the reactor decay heat by the IAEA [55].

As can be observed in Table II the relative uncertainty in  $I_\beta^0$  obtained by TAGS spectrum deconvolution is rather large in these four cases. In particular in the case of  $^{100\text{gs}}\text{Nb}$ , estimated to be one of the largest contributors in the region of the spectral distortion around 5 MeV, reaches 35%. In the case of  $^{102\text{m}}\text{Nb}$  it is 24%. In both cases the TAGS analysis is strongly affected by the uncertainty in the contamination of the parent activity (see Ref. [26] for more details). The characteristic of the  $4\pi\gamma - \beta$  method of being almost insensitive to the actual  $\beta$ -intensity distribution obtained in the TAGS analysis can be of advantage here.

As can be seen in Table II an overall good agreement is found between the g.s. feeding probabilities obtained with the  $4\pi\gamma - \beta$  method and those determined in the TAGS analyses. The  $4\pi\gamma - \beta$  method, however, produces results with much smaller relative uncertainties compared to the TAGS analysis for the two Nb cases: 15% and 6% respectively. Smaller uncertainties are also obtained for  $^{137}\text{I}$  and  $^{140}\text{Cs}$ . The central values are in agreement within uncertainties for both methods. However, observing all the values in the Table II one could

also claim that the  $4\pi\gamma - \beta$  method tends to produce results systematically smaller than TAGS spectrum deconvolution, with the exception of  $^{102\text{m}}\text{Nb}$ . Whether this is true and could be related to some systematic error in one of the two methods should be studied further.

Compared to the values in the ENSDF database [30] we observe (see Table II) that the  $4\pi\gamma - \beta$  method is in close agreement for  $^{137}\text{I}$  and  $^{140}\text{Cs}$ , and 20% smaller for  $^{100\text{gs}}\text{Nb}$  although in agreement within uncertainties. No value is available for  $^{102\text{m}}\text{Nb}$  in the ENSDF database.

## V. SUMMARY AND CONCLUSIONS

In this work we have addressed the determination of the  $\beta$ -decay intensity to the g.s. of the daughter nucleus  $I_\beta^0$  by means of a  $\beta$ - $\gamma$  counting method. This approach, initially proposed by Greenwood *et al.* [2], relies on the use of a high-efficiency  $\gamma$  calorimeter in coincidence with a  $\beta$  detector. The original  $4\pi\gamma - \beta$  method has been revised and some inconsistencies in the formulas were found and corrected. Furthermore we extended the formulas to the particular case of  $\beta$ -delayed neutron emitters, to take into account the fraction of decays proceeding by neutron emission. We have shown that the method becomes an extension of and relies on the total absorption  $\gamma$ -ray spectroscopy technique. The analysis performed using this technique provides the information needed to calculate the quantities required by the  $4\pi\gamma - \beta$  method as well as the accurate determination of contaminant contributions, which results in an improved overall accuracy. The robustness of the method is demonstrated using synthetic decay data obtained from MC simulations. It was shown that statistics becomes a limiting factor for determining with precision the decay probability to the g.s. as this probability becomes smaller.

We have applied the  $4\pi\gamma - \beta$  method to a number of cases measured in our last experimental campaign with the DTAS spectrometer at the IGISOL IV facility. The main goal of the campaign was to measure accurately the  $\beta$ -intensity distribution in the decay of FP of importance in determining the antineutrino spectrum and the decay heat from reactors, several of which have a large decay to the g.s. The TAGS analysis of one case,  $^{103}\text{Tc}$ , turned out to be insensitive to the value of the g.s. feeding probability, and the  $4\pi\gamma - \beta$  counting method was the only way to determine its rather large value of about 45%. Even though  $^{103}\text{Tc}$  is a special case, this shows one of the potential issues when determining the g.s.  $\beta$ -decay intensity from the deconvolution method. For the remaining cases, with  $I_\beta^0$  values ranging from 0 to more than 90%, good agreement between the g.s. feeding probabilities determined in the TAGS analysis and those obtained with the  $4\pi\gamma - \beta$  method was observed. This provides a confirmation of previous g.s. feeding probabilities obtained by the TAGS deconvolution method and in particular confirms the accuracy of the simulation of the shape of the  $\beta$  penetration, to which the  $4\pi\gamma - \beta$  method is not sensitive. For the cases studied we found that, with the exception of the negligible intensity of  $^{95}\text{Rb}$ , the uncertainties in the  $4\pi\gamma - \beta$  method are smaller. Besides case-specific reasons this is related to the small effect of our lack of knowledge of level deexcitations in the daughter

nucleus on this method, whilst it represents a significant fraction of the error budget in the TAGS analysis. In particular the uncertainties for the important contributors to the reactor antineutrino spectrum  $^{100\text{gS}}\text{Nb}$  and  $^{102\text{m}}\text{Nb}$  are reduced by factors 2.5 and 4, respectively, resulting in more precise antineutrino spectra for these nuclei with a corresponding improvement in future summation calculations.

In conclusion, the  $4\pi\gamma - \beta$  method represents an alternative, generally superior, approach to the TAGS spectrum deconvolution to determine g.s. feeding probabilities. The potential of this tool to provide accurate and precise  $I_{\beta}^0$  values, which is hampered by the lack of associated  $\gamma$ -ray emission, was demonstrated in this work. g.s. feeding probabilities are needed to determine the absolute value of the decay intensity to excited states and carry important information on the nuclear structure. In addition, due to the significant influence of the  $\beta$ -decay branches to the g.s. on the reactor antineutrino spectrum and decay heat, our capacity to better determine such transitions will help us understand the challenging puzzle of reactor antineutrinos, while improving decay heat predictions.

#### ACKNOWLEDGMENTS

This work has been supported by the Spanish Ministerio de Economía y Competitividad under Grants No. FPA2011-24553, No. AIC-A-2011-0696, No. FPA2014-52823-C2-1-P, No. FPA2015-65035-P, No. FPI/BES-2014-068222,

No. FPA2017-83946-C2-1-P, and No. RTI2018-098868-B-I00 and the program Severo Ochoa (SEV-2014-0398); by the Spanish Ministerio de Educación under Grant No. FPU12/01527; by the Spanish Ministerio de Ciencia e Innovación under Grant No. PID2019-104714GB-C21; by the European Commission under CHANDA project funded under FP7-EURATOM-FISSION Grant No. 605203; the FP7/ENSAR Contract No. 262010; the SANDA project funded under H2020-EURATOM-1.1 Grant No. 847552; the Horizon 2020 research and innovation programme under Grant No. 771036 (ERC CoG MAIDEN); by the Generalitat Valenciana regional funds PROMETEO/2019/007/; and by the *Junta para la Ampliación de Estudios* Programme (CSIC JAE-Doc contract) co-financed by ESF. We acknowledge the support of the UK Science and Technology Facilities Council (STFC) Grant No. ST/P005314/1; of the Polish National Agency for Academic Exchange (NAWA) under Grant No. PPN/U LM/2019/1/00220; and of the National Science Center, Poland, under Contract No. 2019/35/D/ST2/02081. This work was also supported by the Academy of Finland under the Finnish Centre of Excellence Programme (Project No. 213503, Nuclear and Accelerator-Based Physics Research at JYFL). A.K. and T.E. acknowledge support from the Academy of Finland under Projects No. 275389 and No. 295207, respectively. This work has also been supported by the CNRS challenge NEEDS and the associated NACRE project, the CNRS/in2p3 PICS TAGS between Subatech and IFIC, and the CNRS/in2p3 Master projects Jyväskylä and OPALE.

- 
- [1] J. C. Hardy *et al.*, *Phys. Lett. B* **71**, 307 (1977).  
 [2] R. C. Greenwood *et al.*, *Nucl. Instrum. Methods A* **317**, 175 (1992).  
 [3] B. Rubio *et al.*, *J. Phys. G* **31**, S1477 (2005).  
 [4] R. C. Greenwood *et al.*, *Nucl. Instrum. Methods A* **356**, 385 (1995).  
 [5] R. C. Greenwood *et al.*, *Nucl. Instrum. Methods A* **378**, 312 (1996).  
 [6] C. L. Duke *et al.*, *Nucl. Phys. A* **151**, 609 (1970).  
 [7] A. A. Byklov, V. D. Witman, F. V. Moroz, and Y. V. Naumov, *Izv. Akad. Nauk SSSR, Ser. Fiz.* **44**, 918 (1980).  
 [8] R. C. Greenwood *et al.*, *Nucl. Instrum. Methods A* **314**, 514 (1992).  
 [9] M. Karny *et al.*, *Nucl. Instrum. Methods B* **126**, 411 (1997).  
 [10] J. L. Tain and D. Cano-Ott, *Nucl. Instrum. Methods A* **571**, 728 (2007).  
 [11] D. Cano-Ott *et al.*, *Nucl. Instrum. Methods A* **430**, 333 (1999).  
 [12] S. Agostinelli *et al.*, *Nucl. Instrum. Methods A* **506**, 250 (2003).  
 [13] F. Wauters *et al.*, *Nucl. Instrum. Methods A* **609**, 156 (2009).  
 [14] J. L. Tain *et al.*, *J. Kor. Phys. Soc.* **59**, 1499 (2011).  
 [15] J. L. Tain *et al.*, *Nucl. Instrum. Methods A* **803**, 36 (2015).  
 [16] M. Karny *et al.*, *Nucl. Instrum. Methods A* **836**, 83 (2016).  
 [17] A. Algora *et al.*, *Phys. Rev. Lett.* **105**, 202501 (2010).  
 [18] D. Jordan *et al.*, *Phys. Rev. C* **87**, 044318 (2013).  
 [19] D. D. Frenne *et al.*, *Nucl. Data Sheets* **110**, 1745 (2009).  
 [20] A.-A. Zakari-Issoufou *et al.*, *Phys. Rev. Lett.* **115**, 102503 (2015).  
 [21] E. Valencia *et al.*, *Phys. Rev. C* **95**, 024320 (2017).  
 [22] B. C. Rasco *et al.*, *Phys. Rev. Lett.* **117**, 092501 (2016).  
 [23] A. Fijałkowska *et al.*, *Phys. Rev. Lett.* **119**, 052503 (2017).  
 [24] V. Guadilla *et al.*, *Phys. Rev. C* **96**, 014319 (2017).  
 [25] S. Rice *et al.*, *Phys. Rev. C* **96**, 014320 (2017).  
 [26] V. Guadilla *et al.*, *Phys. Rev. C* **100**, 024311 (2019).  
 [27] V. Guadilla *et al.*, *Phys. Rev. C* **100**, 044305 (2019).  
 [28] R. W. King and J. F. Perkins, *Phys. Rev.* **112**, 963 (1958).  
 [29] A. A. Sonzogni, T. D. Johnson, and E. A. McCutchan, *Phys. Rev. C* **91**, 011301(R) (2015).  
 [30] ENSDF database <http://www.nndc.bnl.gov/ensdf>.  
 [31] M. Wang *et al.*, *Chin. Phys. C* **41**, 030003 (2017).  
 [32] C. Banglin, *Nucl. Data Sheets* **91**, 423 (2000).  
 [33] C. Banglin, *Nucl. Data Sheets* **113**, 2187 (2012).  
 [34] G. Lhersonneau *et al.*, *Phys. Rev. C* **74**, 017308 (2006).  
 [35] K. Schreckenbach *et al.*, *Phys. Lett. B* **99**, 251 (1981).  
 [36] T. A. Mueller *et al.*, *Phys. Rev. C* **83**, 054615 (2011).  
 [37] P. Huber, *Phys. Rev. C* **84**, 024617 (2011).  
 [38] G. Mention, M. Fechner, T. Lasserre, T. A. Mueller, D. Lhuillier, M. Cribier, and A. Letourneau, *Phys. Rev. D* **83**, 073006 (2011).  
 [39] P. Vogel *et al.*, *Nat. Commun.* **6**, 6935 (2015).  
 [40] M. Estienne *et al.*, *Phys. Rev. Lett.* **123**, 022502 (2019).  
 [41] F. P. An *et al.*, *Phys. Rev. Lett.* **116**, 061801 (2016).  
 [42] Y. Abe *et al.*, *Phys. Rev. Lett.* **108**, 131801 (2012).  
 [43] J. K. Ahn *et al.*, *Phys. Rev. Lett.* **108**, 191802 (2012).

- [44] A. C. Hayes, J. L. Friar, G. T. Garvey, D. Ibeling, G. Jungman, T. Kawano, and R. W. Mills, *Phys. Rev. D* **92**, 033015 (2015).
- [45] A. A. Sonzogni, M. Nino, and E. A. McCutchan, *Phys. Rev. C* **98**, 014323 (2018).
- [46] T. D. Johnson and W. D. Kulpa, *Nucl. Data Sheets* **129**, 1 (2015).
- [47] E. A. McCutchan and A. A. Sonzogni, *Nucl. Data Sheets* **115**, 135 (2014).
- [48] D. Abriola, B. Singh, and I. Dillmann, IAEA Report No. INDC(NDS)-0599, IAEA, Vienna, Austria, 2011.
- [49] J. L. Tain and D. Cano-Ott, *Nucl. Instrum. Methods A* **571**, 719 (2007).
- [50] I. D. Moore *et al.*, *Nucl. Instrum. Methods B* **317**, 208 (2013).
- [51] V. Guadilla *et al.*, *Nucl. Instrum. Methods B* **376**, 334 (2016).
- [52] V. Guadilla *et al.*, *Nucl. Instrum. Methods A* **910**, 79 (2018).
- [53] V. Guadilla *et al.*, *Phys. Rev. Lett.* **122**, 042502 (2019).
- [54] D. Cano-Ott *et al.*, *Nucl. Instrum. Methods A* **430**, 488 (1999).
- [55] P. Dimitriou and A. L. Nichols, IAEA Report No. INDC(NDS)-0676, IAEA, Vienna, Austria, 2015.
- [56] H. Niizeki *et al.*, *J. Phys. Soc. Jpn.* **47**, 26 (1979).
- [57] V. Guadilla *et al.*, *Acta Phys. Pol. B* **48**, 529 (2017).
- [58] D. D. Frene, *Nucl. Data Sheets* **110**, 2081 (2009).
- [59] J. K. Dickens and J. W. McConnell, *Phys. Rev. C* **23**, 331 (1981).
- [60] V. Guadilla *et al.*, *Nucl. Instrum. Methods A* **854**, 134 (2017).